⌘ *Author's Choice*

THE JOURNAL OF BIOLOGICAL CHEMISTRY VOL. 286, NO. 29, pp. 26198–26209, July 22, 2011
© 2011 by The American Society for Biochemistry and Molecular Biology, Inc. Printed in the U.S.A.

Forkhead-associated (FHA) Domain Containing ABC Transporter Rv1747 Is Positively Regulated by Ser/Thr Phosphorylation in *Mycobacterium tuberculosis*[*] [S]

Received for publication, March 31, 2011, and in revised form, May 24, 2011 Published, JBC Papers in Press, May 26, 2011, DOI 10.1074/jbc.M111.246132

Vicky L. Spivey[‡1], Virginie Molle[§2], Rachael H. Whalan[‡3], Angela Rodgers[¶], Jade Leiba[§], Lasse Stach[‖], K. Barry Walker[¶], Stephen J. Smerdon[‖], and Roger S. Buxton[‡4]

From the [‡]Division of Mycobacterial Research, Medical Research Council National Institute for Medical Research, Mill Hill, London NW7 1AA, United Kingdom, the [§]Laboratoire de Dynamique des Interactions Membranaires Normales et Pathologiques, Universités de Montpellier II et I, CNRS, UMR 5235, Case 107, Place Eugène Bataillon, 34095 Montpellier Cedex 05, France, the [¶]Immunology and Cellular Immunity Section, Bacteriology Division, National Institute of Biological Standards and Control (A Centre of the Health Protection Agency), Blanche Lane, South Mimms, Potters Bar, Hertfordshire EN6 3QG, United Kingdom, and the [‖]Division of Molecular Structure, Medical Research Council National Institute for Medical Research, Mill Hill, London NW7 1AA, United Kingdom

One major signaling method employed by *Mycobacterium tuberculosis*, the causative agent of tuberculosis, is through reversible phosphorylation of proteins mediated by protein kinases and phosphatases. This study concerns one of these enzymes, the serine/threonine protein kinase PknF, that is encoded in an operon with Rv1747, an ABC transporter that is necessary for growth of *M. tuberculosis in vivo* and contains two forkhead-associated (FHA) domains. FHA domains are phosphopeptide recognition motifs that specifically recognize phosphothreonine-containing epitopes. Experiments to determine how PknF regulates the function of Rv1747 demonstrated that phosphorylation occurs on two specific threonine residues, Thr-150 and Thr-208. To determine the *in vivo* consequences of phosphorylation, infection experiments were performed in bone marrow-derived macrophages and in mice using threonine-to-alanine mutants of Rv1747 that prevent specific phosphorylation and revealed that phosphorylation positively modulates Rv1747 function *in vivo*. The role of the FHA domains in this regulation was further demonstrated by isothermal titration calorimetry, using peptides containing both phosphothreonine residues. FHA-1 domain mutation resulted in attenuation in macrophages highlighting the critical role of this domain in Rv1747 function. A mutant deleted for *pknF* did not, however, have a growth phenotype in an infection, suggesting that other kinases can fulfill its role when it is absent. This study provides the first information on the molecular mechanism(s) regulating Rv1747 through PknF-dependent phosphorylation but also indicates that phosphorylation activates Rv1747, which may have important consequences in regulating growth of *M. tuberculosis*.

Tuberculosis (TB),[5] caused by *Mycobacterium tuberculosis*, remains one of the world's most rampant infective agents, and despite preventative and therapeutic measures, this pathogen killed 1.8 million people in 2008 alone. Furthermore, an estimated two billion people are latently infected with TB bacilli (1). Globally, this disease burden has escalated because of its deadly synergy with human immunodeficiency virus (HIV). This HIV burden coupled with the emergence and increase of multidrug and extensively drug-resistant *M. tuberculosis* strains have made the search for new TB drugs ever more important.

Signal transduction in *M. tuberculosis* has become a target for the development of novel therapeutics in the treatment of TB. Protein kinases and phosphatases allow reversible protein phosphorylation to transduce extracellular signals into cellular responses, and this has been implicated in nearly all basic cellular processes (2). Consequently, small molecule kinase inhibitors represent attractive candidates as drug targets (3, 4). *M. tuberculosis* has a repertoire of both the classical bacterial two-component systems involving histidine kinases and response regulators and also a second family comprising the serine/threonine protein kinases (STPKs), a system originally thought to be only present in eukaryotes. Studies performed to date have demonstrated the presence of a complex network of phosphorylation-dependent interactions mediated by STPKs in *M. tuberculosis* (5–7). A total of 11 STPKs have been identified (8, 9), significantly 4 of which lie in putative operons with forkhead-associated (FHA) domain-containing proteins.

FHA domains are modular phosphopeptide recognition motifs, conserved from bacteria to humans, which are between 95 and 150 amino acid residues in size and demonstrate a strik-

* This work was supported by Medical Research Council studentships (to V. L. S. and L. S.), Medical Research Council Grants U117585867 and U117584228, National Research Agency Grants ANR-06-MIME-027-01 and ANR-09-MIEN-004, and by the Health Protection Agency.

[S] The on-line version of this article (available at http://www.jbc.org) contains supplemental Fig. S1.

⌘ *Author's Choice*—Final version full access.

[1] Present address: School of Biosciences, University of Birmingham, Edgbaston, Birmingham B15 2TT, United Kingdom.

[2] To whom correspondence may be addressed. Tel.: 33-4-67-14-47-25; Fax: 33-4-67-14-42-86; E-mail: virginie.molle@univ-montp2.fr.

[3] Present address: Eastman Dental Institute, 256 Gray's Inn Rd., London WC1X 8LD, United Kingdom.

[4] To whom correspondence may be addressed. Tel.: 44-20-8816-2225; Fax: 44-20-8906-4477; E-mail: rbuxton@nimr.mrc.ac.uk.

[5] The abbreviations used are: TB, tuberculosis; FHA, forkhead-associated; STPK, serine/threonine protein kinase; BMDM, bone marrow-derived macrophage.

ing specificity for phosphothreonine (Thr(P))-containing epitopes (10–12). A total of six FHA-containing proteins have been found encoded within the *M. tuberculosis* genome (9). Rv1747, a predicted ATP-binding cassette (ABC) transporter, encodes two FHA domains, a feature unique to the FHA modules of *M. tuberculosis*. The presence of an FHA domain is now indicative that the protein is likely to interact with a phosphorylated protein partner (13). ABC transporters bind and hydrolyze ATP providing energy for uptake or export of a diverse array of substrates across cell membranes. Rv1747 is a presumed ABC exporter required for the growth of *M. tuberculosis in vivo* (14, 15) and forms a putative operon with its upstream adjacent gene, *pknF,* encoding a Ser/Thr protein kinase. A number of recent investigations have examined phosphorylation by Ser/Thr protein kinases *in vitro* and have identified substrates based on these assays. Thus, previous studies have demonstrated that PknF can phosphorylate the FHA domains of two other proteins, Rv0020c and Rv1747 (16), and also the heat-shock protein GroEL1 (17). Furthermore, PknF has previously been implicated in regulating glucose uptake in *M. tuberculosis* (18), as well as in sliding motility and biofilm formation in *Mycobacterium smegmatis* (19). Thus, mycobacterial Ser/Thr protein kinases have been identified as promising therapeutic targets. However, for a kinase to be a suitable drug target, it is necessary not only to identify a target for the kinase that is required for the growth of the bacterium but also to determine the functional consequences of phosphorylating the target protein. We have therefore sought to combine the approach of analyzing the molecular details of Ser/Thr-mediated phosphorylation with *in vivo* studies designed to elucidate what functional consequences flow from PknF-mediated phosphorylation.

In previous studies, we and others showed that Rv1747 exhibited ATPase activity and was a substrate for PknF *in vitro*; furthermore, the FHA domains of Rv1747 were shown to be required for specific interaction with PknF in a yeast two-hybrid assay (15, 20). Moreover, we demonstrated that deletion of *Rv1747* results in a growth defect in macrophage and mouse infections (15). However, whether phosphorylation is directly involved in regulating Rv1747 function *in vivo* has not been clearly established. This study was undertaken to determine whether Rv1747 function might be influenced by STPK-dependent regulatory mechanisms and how PknF could modulate Rv1747. Therefore, we have characterized Rv1747 phosphorylation sites to decipher how the PknF-Rv1747 signal transduction system functions in *M. tuberculosis*. Then, through the use of mutants in macrophage and mouse infections, we provide for the first time evidence that phosphorylation of Rv1747 is required for its function, *i.e.* phosphorylation positively regulates Rv1747 function.

EXPERIMENTAL PROCEDURES

Strains, Growth Conditions, and Reagents—M. tuberculosis H37Rv cultures were grown at 37 °C in Dubos broth supplemented with 0.05% (v/v) Tween 80, 0.2% (v/v) glycerol, and 4% (v/v) Dubos medium albumin (BD Biosciences). *M. tuberculosis* liquid cultures were grown in 50-ml Falcon tubes in a wheel at 20 rpm (Corning Glass) or in 1,000-ml polycarbonate roller bottles (Nalgene) in a Bellco roll-in incubator (2 rpm). Kanamycin and hygromycin were used at a final concentration of 25 and 50 μg/ml, respectively. *M. tuberculosis* was grown on 7H11 agar plates supplemented with 10% Middlebrook oleic acid-albumin-dextrose-catalase enrichment and 0.5% (v/v) glycerol. All *Escherichia coli* strains (Table 1) were grown on L-agar and in L-broth overnight at 37 °C, with shaking for liquid cultures (250 rpm). Kanamycin and ampicillin were used at a final concentration of 50 and 100 μg/ml, respectively. Adult (6–8 weeks old) female BALB/c mice were obtained from the Biological Services specific pathogen-free animal facility at the National Institute for Medical Research.

RNA Isolation from M. tuberculosis Liquid Cultures—Total RNA was isolated from 100 ml of exponential phase (A_{600} 0.6) rolling cultures using the Fast RNA Pro Blue kit (Qbiogene). Contaminating DNA was removed by DNase digestion with 2 units of RNase-free DNase (Promega) in 5 mM magnesium sulfate and 100 mM sodium acetate with 80 units of RNase inhibitor and incubated at 37 °C for 1 h. A further 2 units of RNase-free DNase was then added and incubated as described previously. Proteins and other contaminants were then removed from RNA samples using the RNeasy kit (Qiagen) as per the manufacturer's guidelines. 200 ng of RNA was then run on a 2100 Bioanalyzer (Agilent Technologies) to assess integrity.

Reverse-transcription PCR (RT-PCR)—A reverse transcription reaction contained 1 μg of DNA-free RNA in 1× Quantiscript RT buffer containing magnesium and dNTPs, RT primer mix, and 1 μl of Quantiscript reverse transcriptase (Qiagen). Reactions were incubated at 42 °C for 30 min. Samples were then incubated at 95 °C for 3 min to inactivate the reverse transcriptase enzyme. PCR was then performed using the cDNA template with HotStarTaq as per the manufacturer's guidelines (Qiagen). Primers used in the RT-PCR study can be found in Table 2.

Cloning, Expression, and Purification of Recombinant PknF and Rv1747 Proteins—The kinase domain of PknF and the nucleotide binding domain along with FHA-1 and FHA-2 domains of Rv1747 were amplified by PCR using *M. tuberculosis* H37Rv chromosomal DNA as a template and ligated into pGEX-6P-1. Full-length proteins were not purified because of the presence of single or multiple transmembrane domains. All plasmids were verified using DNA sequencing. All constructs were expressed as 3C protease-cleavable GST fusions in *E. coli* BL21 (DE3) Star competent cells (Invitrogen) or *E. coli* BL21 (DE3) pRep4 cells as follows. Recombinant strains harboring the different constructs were used to inoculate 4 liters of LB medium supplemented with ampicillin, and the resulting cultures were incubated at 37 °C with shaking until the A_{600} reached 0.6. Isopropyl 1-thio-β-D-galactopyranoside was then added at a final concentration of 0.1 mM, and growth was continued for 16 h at 18 °C. Cells were harvested by centrifugation, washed in PBS plus 10% glycerol, and then resuspended in lysis buffer (50 mM Tris/HCl, pH 8.0, 300 mM NaCl, 10% glycerol) containing DNase, RNase, lysozyme, and a mixture of protease inhibitors (Roche Applied Science). Bacteria were disrupted by sonication (VibraCell, Sonics) on ice with 10 bursts of ~20 s at amplitude 10. The soluble lysate was applied to an appropriate amount of prepared glutathione-Sepharose 4B resin (3–5 ml)

TABLE 1
Bacterial strains and plasmids used in this study

Strains or plasmids	Genotype or description	Source or Ref.
***E. coli* strains**		
E. coli TOP10	F$^-$ *mcr*A Δ(*mrr-hsd*RMS-*mcr*BC) φ80*lacZ*Δ*M15* Δ*lacX74 deoR recA1 araD139* Δ(*ara-leu*)7697 *galU galK rpsL endA1 nupG*; used for general cloning	Invitrogen
E. coli BL21(DE3)Star	F$^-$ *omp*T *hsd*SB(r_B^-, m_B^-)*gal dcm rne*131(DE3); used to express recombinant proteins in *E. coli*	Stratagene
E. coli BL21(DE3)Star pRep4-*groESL*	*E. coli* BL21(DE3)Star plus pRep4-*groESL* plasmid. Expresses GroES and GroEL to increase protein solubility and yield; used to express recombinant proteins in *E. coli*	44
XL1-Blue	*recA1 endA1 gyrA96 thi-1 hsdR17*(r_K^- m_K^+) *supE44 relA1 lac* [F′::Tn10 *proAB*$^+$ *lacI*^{q}*Z*Δ*M15*]; used for site-directed mutagenesis	Stratagene
***M. tuberculosis* strains**		
H37Rv	*M. tuberculosis* WT strain	45
Δ*Rv1747*	H37Rv with deletion of *Rv1747* constructed by homologous recombination with targeting construct pRW69	15
Rv1747 complement	Δ*Rv1747* containing complementing plasmid pRW76	15
Rv1747 complement T150A/T208A	Δ*Rv1747* containing complementing plasmid pRW76 with mutations T150A and T208A	This study
Rv1747 complement S47A	Δ*Rv1747* containing complementing plasmid pRW76 with mutation S47A	This study
Rv1747 complement S248A	Δ*Rv1747* containing complementing plasmid pRW76 with mutation S248A	This study
Δ*pknF*	H37Rv with deletion of *pknF* constructed by homologous recombination with targeting construct pRW51	This study
pknF complement	Δ*pknF* containing complementing plasmid pRW95	This study
***M. tuberculosis* shuttle plasmids**		
p2Nil	Suicide gene delivery vector, *oriE,* Kan^R	22
pKP186	Integrase negative derivative of the integrating vector pMV306, Kan^R	46
pBS-Int	Suicide vector containing integrase, Amp^R	25
pRW69	p2Nil containing a 2-kb region of H37Rv DNA flanking each side of the *Rv1747* gene, Hyg^R	15
pRW76	*Rv1747* complementing plasmid. pKP186 derivative containing 609 bp *Rv1745c*, *pknF,* and *Rv1747*, Kan^R Hyg^R	15
pRW51	p2Nil containing a 3-kb region of H37Rv DNA flanking each side of the *pknF* gene, Kan^R	This study
pRW95	*pknF* complementing plasmid. pKP186 derivative containing 609 bp *Rv1745c*, *pknF,* and 20 bp *Rv1747*, Kan^R	This study
***E. coli* plasmids**		
pGEX-6P-1	Replicating protein expression vector. N-terminal GST tag, *tac* promoter, *lacI* repressor, Amp^R	GE Healthcare
pVS_02	pGEX-6P-1 containing PknF$^{1-292}$	This study
pVS_03	pGEX-6P-1 containing Rv1747$^{1-559}$	This study
pVS_04	pGEX-6P-1 containing FHA-1$^{1-120}$	This study
pVS_05	pGEX-6P-1 containing FHA-2$^{202-310}$	This study
pVS_06	pGEX-6P-1 containing FHA-1$^{1-120}$ S47A	This study
pVS_07	pGEX-6P-1 containing Rv1747$^{1-559}$ T150A	This study
pVS_09	pGex-6P-1 containing Rv1747$^{1-559}$ T208A	This study
pVS_11	pGex-6P-1 containing Rv1747$^{1-559}$ T150A/T208A	This study

(GE Healthcare) equilibrated in lysis buffer. Resin was incubated overnight at 4 °C with gentle mixing. The resin was collected and then washed with 1 liter of wash buffer (50 mM Tris/HCl, pH 8.0, 500 mM NaCl, 10% glycerol). Washed resin was equilibrated with PreScission protease cleavage buffer (50 mM Tris, pH 8.0, 200 mM NaCl, 1 mM EDTA, 0.5 mM DTT, 10% glycerol). 50 μl of PreScission protease was then added to the resin and incubated overnight with mixing as described previously. Elutions were concentrated in a 20-ml Vivaspin ultrafiltration concentrator (VivaScience) with an appropriate molecular weight cutoff filter (3–10 kDa). Each sample was purified by size exclusion chromatography with a pre-packed HiLoad 16/60 Superdex 200 prep grade column (GE Healthcare) using an AKTA Prime system. The column was equilibrated in gel filtration buffer (40 mM Tris/HCl, pH 8.0, 200 mM NaCl, 10% glycerol); the sample was loaded, and the column was developed at flow rates between 0.5 and 1 ml/min collecting fractions. Appropriate fractions containing the protein of interest were checked by SDS-PAGE, pooled, concentrated, and snap-frozen at −80 °C in 20–100-μl aliquots.

In Vitro Phosphorylation Assays—*In vitro* phosphorylation was carried out in 20-μl reactions containing the recombinant PknF (1 μg), Rv1747 derivatives (5 μg), and 200 μCi/ml (65 nM) [γ-^{32}P]ATP (3000 Ci/mmol, PerkinElmer Life Sciences) in phosphorylation buffer (25 mM Tris/HCl, pH 6.8, 1 mM DTT, 5 mM $MgCl_2$, 1 mM EDTA). The reaction was carried out for 30 min at 37 °C and stopped by addition of Laemmli Sample Loading Buffer and incubated at 100 °C for 5 min before analysis by SDS-PAGE. After electrophoresis, gels were washed in 10% trichloroacetic acid for 10 min at 90 °C, stained with InstantBlue Coomassie stain (Expedeon) or dried on a Gel Drier (Savant, Slab Drier), then exposed to a phosphorimager screen (GE Healthcare), and developed on a Storm Scanner (Amersham Biosciences).

Mass Spectrometry Analysis—Purified WT and mutant Rv1747 proteins were subjected to *in vitro* phosphorylation by PknF as described above, except that [γ-^{32}P]ATP was replaced with 5 mM cold ATP. Subsequent analyses using nanoLC/nanospray/tandem mass spectrometry (LC-ESI/MS/MS) were performed as described previously (21).

Generation of the pknF and Rv1747 Deletion and Complementing Strains—The *pknF* (*Rv1746*) null strain was generated as an in-frame unmarked deletion to avoid downstream polar effects on the *Rv1747* gene. The targeting construct was made by the method of PCR-ligation-PCR. 1.5-Kilobase regions of H37Rv DNA flanking each side of the *pknF* gene were PCR-amplified using *Pfu* Ultra (Stratagene) and separately cloned into pCR4Blunt-TOPO (Invitrogen) and sequenced. The primer pairs for the flanking regions were 5′-ATAAGAATGC-GGCCGCACTGTGTAGCGGGGCAAAACGAC-3′ (5′-NotI restriction site underlined), 5′-GATATCCAACTGCCGGAC-GATGGTGAAGC-3′ (5′-EcoRV site underlined), 5′-ATAA-

TABLE 2
Primers used in this study/for transcript analysis

Primer name	Description	Sequence (5′–3′)[a,b]
Primer pairs used for RT-PCR		
pknF F	Gene-specific internal primer	AACATCCTGATCGCCAATCC
pknF R	Gene-specific internal primer	TTGCAGCGTCGAGCAGTAGG
pknF-Rv1747 F	Co-transcription primer	AAGGCACCAACACCACCATCT
pknF-Rv1747 R	Co-transcription primer	GGACAGGTTGGGCAGGCGTAT
Rv1747 F	Gene-specific internal primer	CGTTCACGCCGAATATGCCT
Rv1747 R	Gene-specific internal primer	CCATGAAGACCGCACCGACA
Rv1747-Rv1748 F	Co-transcription primer	AGGATTCGCATTGGCATCAC
Rv1747-Rv1748 R	Co-transcription primer	GGCTTGTAGCTTGGCCTTGT
Rv1748 F	Gene-specific internal primer	GGCGATCTTGCGTCGGATAG
Rv1748 R	Gene-specific internal primer	GTACGGTCCGGCAACACGAT
Primer pairs used for protein expression constructs into pGex-6P-1		
$PknF^{1-292}$ F	BamHI	GGATCCATGCCGCTCGCGGAAGGTTCG
$PknF^{1-292}$ R	XhoI plus STOP	CTCGAGTCACGGTTGCGACACCCGCGT
$Rv1747^{1-559}$ F	BamHI	GGATCCGTGCCGATGAGCCAACCAGCC
$Rv1747^{1-559}$ R	EcoRI plus STOP	GAATTCTCAGTCGTCGGCGACGGTGCTGAA
$FHA\text{-}1^{1-120}$ F	BamHI	CCGGATCCGTGCCGATGAGCCAACCA
$FHA\text{-}1^{1-120}$ R	EcoRI plus STOP	CCGGATTCTCAGCGTATCGACGTCGTCTG
$FHA\text{-}2^{202-310}$ F	BamHI plus ATG	CCGGATCCATGACTGAGGCGGGAAACCTC
$FHA\text{-}2^{202-310}$ R	EcoRI plus STOP	CCGGATTCTCAGTTCTCTTCACGGCGCGC
Primer pairs used for site-directed mutagenesis of *Rv1747*		
*Rv1747*_T150A	T150A mutation	TACAACAGCTTCCACCGGCC**GCC**ACCCGGATACCCGCCGCTCCGGAGCGGCGGGTATCCGGGT**GGC**GGCC GGTGGAAGCTGTTGTA
*Rv1747*_T208A	T208A mutation	CTGAGGCGGGAAACCTCGCG**GCA**TCGATGATGAAGATCCTGCGCGCAGGATCTTCATCATCGA**TGC**CGCG AGGTTTCCCGCCTCAG
*Rv1747*_S47A	S47A mutation	CGCACACCCCCTGATC**GCC**CGGGCACACCTGCTGCGCAGCAGGTGTGCCCG**GGC**GATCAGGGGGTGTGCG
*Rv1747*_S248A	S248A mutation	CCCGAGGTGTTGGCC**GCA**CGTCACCACGCCACCCGGGTGGCGTGGTGAC**GTG**CGGCCAACACCTCGGG

[a] Underlined bases highlight restriction site.
[b] Boldface bases indicate the change of an amino acid to alanine.

GAATGCGGCCGCTCGGCGACGGTGCTGAAGA-3′ (5′-NotI site underlined), and 5′-GATATCGGCTGGCCG-TGATGGTC-3′(5′-EcoRV site underlined). The fragments were then digested out of pCR4Blunt-TOPO using EcoRV and NotI for the upstream fragment and EcoRV and EcoRI for the downstream fragment (from the multiple cloning site). To generate the fusion between the two PCR products, 5-μl aliquots of each phosphorylated PCR product were mixed, and 1 μl of highly concentrated T4 DNA ligase (2,000 units/μl) (New England Biolabs) was added for 15 min at room temperature. To amplify the fusion gene, 1 μl of the ligation reaction was amplified by PCR using the 5′ primer of the upstream fragment and the 3′ primer of the downstream fragment. The resulting DNA fragment was re-cloned into pCR4Blunt-TOPO and sequenced. It was subsequently digested out using NotI and BamHI and cloned into the *M. tuberculosis* suicide vector p2Nil (22). Finally, the *sacB* and *lacZ* genes were inserted from the plasmid pGOAL17 (22) using PacI. This targeting construct was used to electroporate *M. tuberculosis*. This was plated onto 7H11 plates supplemented with X-Gal and kanamycin and incubated at 37 °C for 3 weeks. Single-crossover events, seen as blue colonies, were streaked onto 7H11 and grown for a further 3 weeks before they were serially diluted and streaked onto 7H11 supplemented with sucrose. The resulting colonies were patch tested on 7H11 plates containing X-Gal or kanamycin to identify white kanamycin-sensitive colonies, indicating a double-crossover event. The resulting colonies were harvested; DNA was extracted, and the colonies were checked by PCR and DNA microarrays to confirm the deletion.

Complementation of the *pknF* deletion was achieved by PCR, amplifying the genes *pknF*, 609 bp of *Rv1745c,* and 20 bp of *Rv1747* using primers 5′-GAATTCGTAACATCGCGCAC-GAATTG-3′ (5′-EcoRI restriction site underlined) and -CCG-GAATTCGCTGGTTGGCTCATC-3′ (5′-EcoRI site) (Fig. 1). The PCR product was then cloned into the vector pKP186 (23), a pMV306 (24) derivative lacking the integrase gene, and used to electroporate the *M. tuberculosis* Δ*pknF* mutant along with the mycobacterial suicide vector, pPS-Int, which contains the integrase gene (Table 1) (15, 25).

The *Rv1747* deletion mutant (hygromycin marked) was described previously (15). Complementation of the *Rv1747* deletion was achieved by PCR, amplifying the genes *Rv1747*, *pknF* (*Rv1746*), and 609 bp of *Rv1745c* using primers 5′-AAGCTTGCACGCCTTGAGGCGAAT CT-3′ (5′HindIII site) and 5′-GAATTCGTAACATCGCGCACGAATTG-3′ (5′ EcoRI site) (15). The PCR product was then cloned into the vector pKP186 and transformed into the *M. tuberculosis* Δ*Rv1747* mutant as above.

Site-directed Mutagenesis—Site-directed mutagenesis was carried out according to the Stratagene QuikChange XL site-directed mutagenesis manual, using SoloPack Gold Supercompetent *E. coli* for transformation. Mutation of the phosphorylated threonine residues of Rv1747 was created by substitution of Thr-150 and Thr-208 with alanine. Sequences of primers used are shown in Table 2. After site-directed mutagenesis, constructs were re-cloned into pKP186 or pGEX-6P-1 to ensure no mutations had occurred within the plasmid backbone (Table 1). The presence of the desired mutations was confirmed by sequencing.

Growth of M. tuberculosis in Murine Bone Marrow-derived Macrophages—Monocytes were isolated from the hind legs of 6–8-week-old female BALB/c mice. The cells were resuspended in 10 ml of RPMI 1640 medium (Invitrogen) supplemented with 10% heat-inactivated fetal calf serum (Invitrogen), 2 mM L-glutamine, 1 mM sodium pyruvate, 10 mM HEPES, and 50 μM β-mercaptoethanol (RPMI complete) in a Petri dish. A

10-ml aliquot of 0.83% ammonium chloride was added for 5 min at 37 °C to lyse the red blood cells. Cells were harvested again, and ammonium chloride was removed. Cells were washed in 10 ml of 1× PBS (Invitrogen) and then resuspended in 10 ml of RPMI complete containing 20% by volume of supernatant from L929 cells that produce macrophage colony-stimulating factor. Monocytes were plated out in Petri dishes at a concentration of 4×10^6 cells per plate in RPMI complete plus 20% L929 supplement in a total volume of 10 ml. Cells were incubated at 37 °C with 5% CO_2. After 72 h, a further 10 ml of RPMI complete plus 20% L929 supplement was added to each Petri dish. After a further 48 h, macrophages were ready to use. All media and nonadherent cells were removed from the Petri dishes. 4 mM EDTA in 1× PBS was added to flush the cells from the plate. The supernatant was discarded, and the cell pellet was resuspended in RPMI complete containing 5% L929 supplement. 2×10^5 macrophages were seeded per well in a 1-ml volume in a 24-well cell culture plate (tissue culture-treated plates, Costar). When required, mouse interferon-γ (IFNγ) was added at 20 ng/ml (Roche Applied Science) to activate the macrophages, and activation was confirmed using the Greiss assay. Cells were plated out in triplicate for each *M. tuberculosis* strain and post-infection time point. Prior to infection, cells were incubated for 18 h at 37 °C with 5% CO_2 to allow adherence and activation. The macrophages were infected with *M. tuberculosis* with a multiplicity of infection of 0.5 bacteria: 1 macrophage for 6 h. Survival and multiplication of *M. tuberculosis* within the macrophages were assessed at 6, 24, 72, 120, and 168 h post-infection. At each time point, medium was removed from each well, and macrophages were lysed in 500 μl of distilled H_2O plus 0.05% Tween 80 for 30 min. Appropriate dilutions of bacteria were then plated onto 7H11 agar plates and incubated at 37 °C for 2–4 weeks. Colonies were then counted and cfu/ml calculated.

Growth of M. tuberculosis in Mice—*M. tuberculosis* cultures were grown in Dubos medium to an A_{600} of 0.6. Cultures were pelleted and resuspended in DMEM (Sigma) plus 2 mM L-glutamine and 50% fetal calf serum to a concentration of 10^9 bacteria per ml. Subsequently, 10-ml bacterial stocks were prepared containing ~10^5 cfu/ml, and mice were infected with ~100 cfu each, using a Glas-Col aerosol infection system. Aerosol infections were performed at the National Institute for Biological Standards and Control. The infection was monitored by removing the lungs and spleens of infected mice at various intervals, homogenizing the tissues, and plating 10-fold serial dilutions to determine numbers of cfu of *M. tuberculosis*. The growth curves were compared by graph and statistical analysis. The results for each time point are the means of cfu determinations performed on organs from five mice, and the error bars show the standard error of the means.

Isothermal Titration Calorimetry—Experiments to determine binding affinities and stoichiometries were performed with the MicroCal iTC_{200} system (GE Healthcare). 200 μl of purified FHA-1 or FHA-2 protein (at 50 μM) in 20 mM Tris/HCl, pH 8, and 150 mM NaCl was loaded into the sample cell. 100 μl of phosphopeptide (at 500 μM) in the same buffer was loaded into the syringe. During the experiment, 2 μl of ligand was titrated into the sample cell every 180 s with a total of 20 injections. The sequence of the synthesized Thr(P)-150 peptide was KKYAGQQLPPApTTRIPAA and the sequence of the Thr(P)-208 peptide was KKYAGTEAGNLApTSMMK, where pT is the phosphothreonine residue.

RESULTS

pknF and Rv1747 Form a Two Gene Operon—The genomic localization of *pknF* and *Rv1747* (Fig. 1*A*) suggested that the two genes could potentially form an operon as the intergenic region between *pknF* and *Rv1747* is only 62 bp. Therefore, to confirm this hypothesis, we performed RT-PCR showing that there was a transcript extending from *pknF* through the intergenic region into *Rv1747*, thus demonstrating that these two genes are indeed co-transcribed (Fig. 1*B*). A transcript was also present for each investigated gene when using gene-specific internal primers, although no transcript was detected in the intergenic region between *Rv1747* and *Rv1748* when using a forward primer within *Rv1747* and with a reverse primer within *Rv1748*, indicating that these two genes are not co-transcribed. In addition, no transcript was present between *Rv1748* and the convergent gene *Rv1749c*. Therefore, these results confirmed that *pknF* and *Rv1747* are co-transcribed. Such co-localization of genes within the same operon is usually taken to indicate that there is a functional relationship between the gene products; this prompted us to study the role of a putative interaction between PknF and Rv1747.

Rv1747 Is Phosphorylated by PknF on Two Threonine Residues—To decipher the role of phosphorylation on Rv1747, it was necessary to determine the PknF-mediated phosphorylation sites. First of all, we confirmed the phosphorylation of Rv1747 by PknF with the recombinant proteins newly generated. Thus, only the kinase domain of PknF (residues 1–292) and the nucleotide binding domain of Rv1747 (residues 1–559) were cloned, expressed, and purified as recombinant proteins from *E. coli*. Phosphorylation of Rv1747 did not occur with PknG and was extremely weak with PknB (supplemental Fig. S1*A*). Using the recombinant proteins, we showed that PknF was an active kinase in an *in vitro* assay and was indeed able to specifically phosphorylate Rv1747, whereas Rv1747 did not have any autophosphorylation activity (Fig. 2*A*), thus confirming our previous results (20). In a second step, a mass spectrometry strategy was used to identify the number and nature of the phosphorylation sites on Rv1747. Such a method has been successfully used to elucidate the phosphorylation sites in a sequence-specific fashion for several *M. tuberculosis* STPK substrates (17, 26–29). Rv1747 was incubated with unlabeled ATP in the presence of PknF and subjected to mass spectrometric analysis after tryptic digestion. Spectral identification and phosphorylation determination were achieved with the paragon algorithm from the ProteinPilot® 2.0 data base-searching software (Applied Biosystems) using the phosphorylation emphasis criterion against our locally constructed data base that included the sequences of Rv1747 and derivatives. The phosphopeptides identified by the software were then validated by manual examination of the corresponding MS/MS spectra. Manual validations were performed based on neutral loss of H_3PO_4 from the precursor ion and the assignment of major fragment ions to b- and y-ion series or to the corresponding

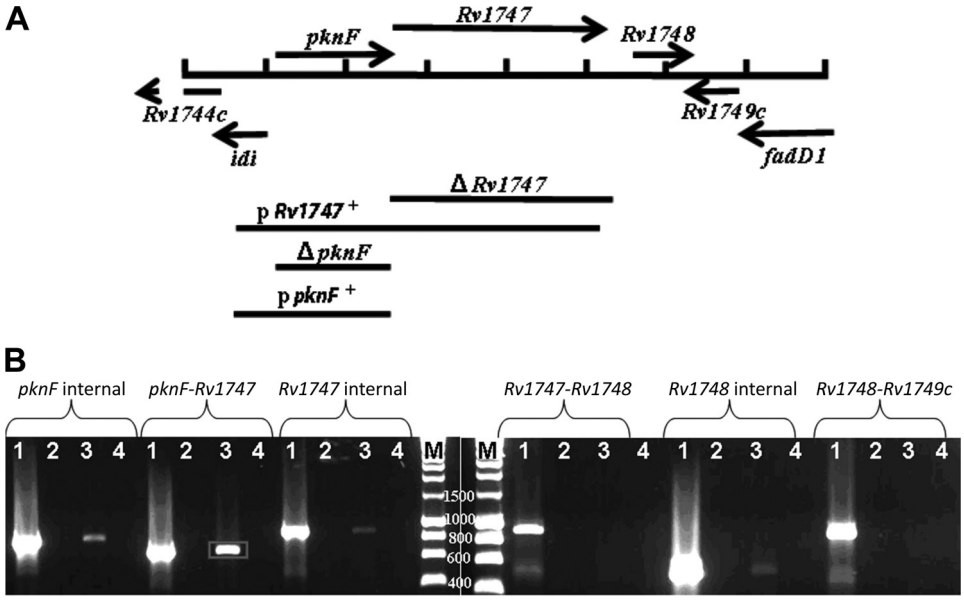

FIGURE 1. *A,* diagram of the genomic region of *M. tuberculosis* containing *pknF* and *Rv1747* genes. The figure shows the extent of the *pknF* and *Rv1747* deletions and the complementing plasmids p*pknF*$^+$ and p*Rv1747*$^+$. The *pknF* deletion was designed as an in-frame deletion strain. The *Rv1747* complementing plasmid included a copy of *pknF*. The marks on the chromosome are at 1,000-bp intervals. *B,* RT-PCR of *pknF* and *Rv1747*. RT-PCR results showing the products of cDNA amplification. 10 μl of a 50-μl RT reaction was analyzed by agarose gel electrophoresis. Labels *above* the gel show the primer pairs used in each PCR (Table 2). *Lane 1* of each primer pair is the positive control (H37Rv genomic DNA). *Lane 2* is a negative control (no mRNA added to the RT reaction). *Lane 3* is the RT-positive lane. *Lane 4* is RT-negative (no reverse transcriptase present in RT reaction). The *pknF-Rv1747* transcript is indicated by a *box*. *M* is the DNA ladder, and the relevant sizes in base pairs are labeled.

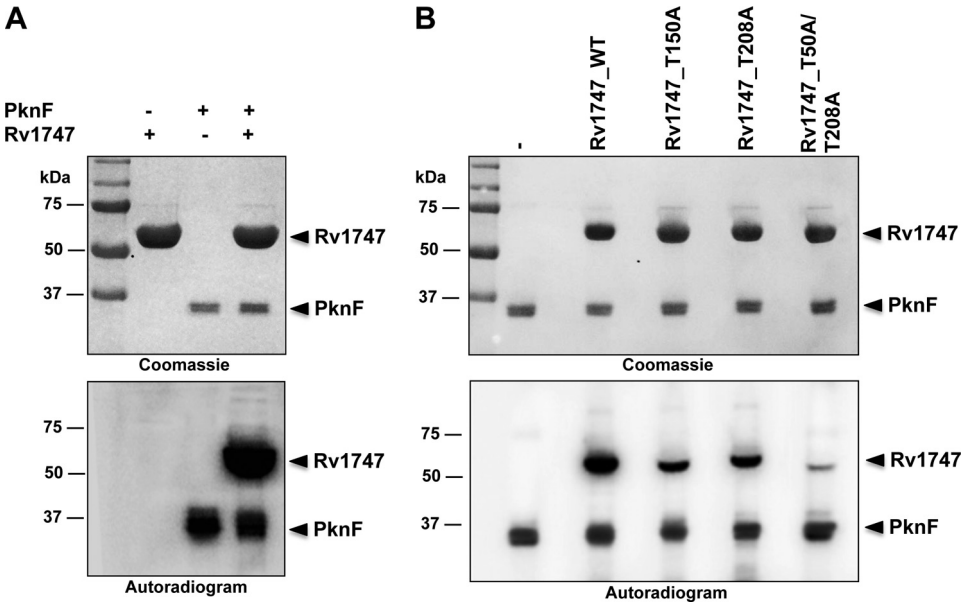

FIGURE 2. *A, in vitro* phosphorylation of *M. tuberculosis* Rv1747 by PknF. The recombinant PknF and Rv1747 proteins were purified as described above, and the GST tag was cleaved from the protein prior to incubation with [γ-^{32}P]ATP. Samples were separated by SDS-PAGE, Coomassie-stained (*upper panel*), and visualized by autoradiography (*lower panel*). Lower bands illustrate the autokinase activity of PknF, whereas upper bands reflect Rv1747 phosphorylation. *B, in vitro* phosphorylation of Rv1747 mutants by PknF. The various Rv1747 mutant proteins were used in phosphorylation assays in equal amounts in the presence of [γ-^{32}P]ATP and PknF. The Rv1747_WT, Rv1747_T150A, Rv1747_T208A, and Rv1747_T150A/T208A mutant proteins were separated by SDS-PAGE and stained with Coomassie Blue (*upper panel*), and the radioactive bands were revealed by autoradiography (*lower panel*). Standard proteins of known molecular masses (in kilodaltons) were run in parallel, and their positions are shown to the *left* of the figures.

neutral loss of H_3PO_4 from these ions. The sequence coverage of the protein was 96% and phosphorylation occurred only on peptides 119–164 and 199–212 as the MS/MS spectra unambiguously confirmed the presence of a phosphate group on Thr-150 and Thr-208 (Fig. 3), which are situated between the FHA-1 and FHA-2 domain for Thr-150, although Thr-208 is just upstream of the FHA-2 domain.

Moreover, to confirm the phosphorylation sites identified, we co-expressed the PknF kinase and its substrate Rv1747 in *E. coli* using a strategy described recently (30). The PknF kinase domain and its cognate substrate Rv1747 were cloned into the pCDF-Duet vector and overexpressed, and therefore the His-tagged phosphorylated Rv1747 was purified as described previously, whereas the PknF kinase was not tagged and therefore

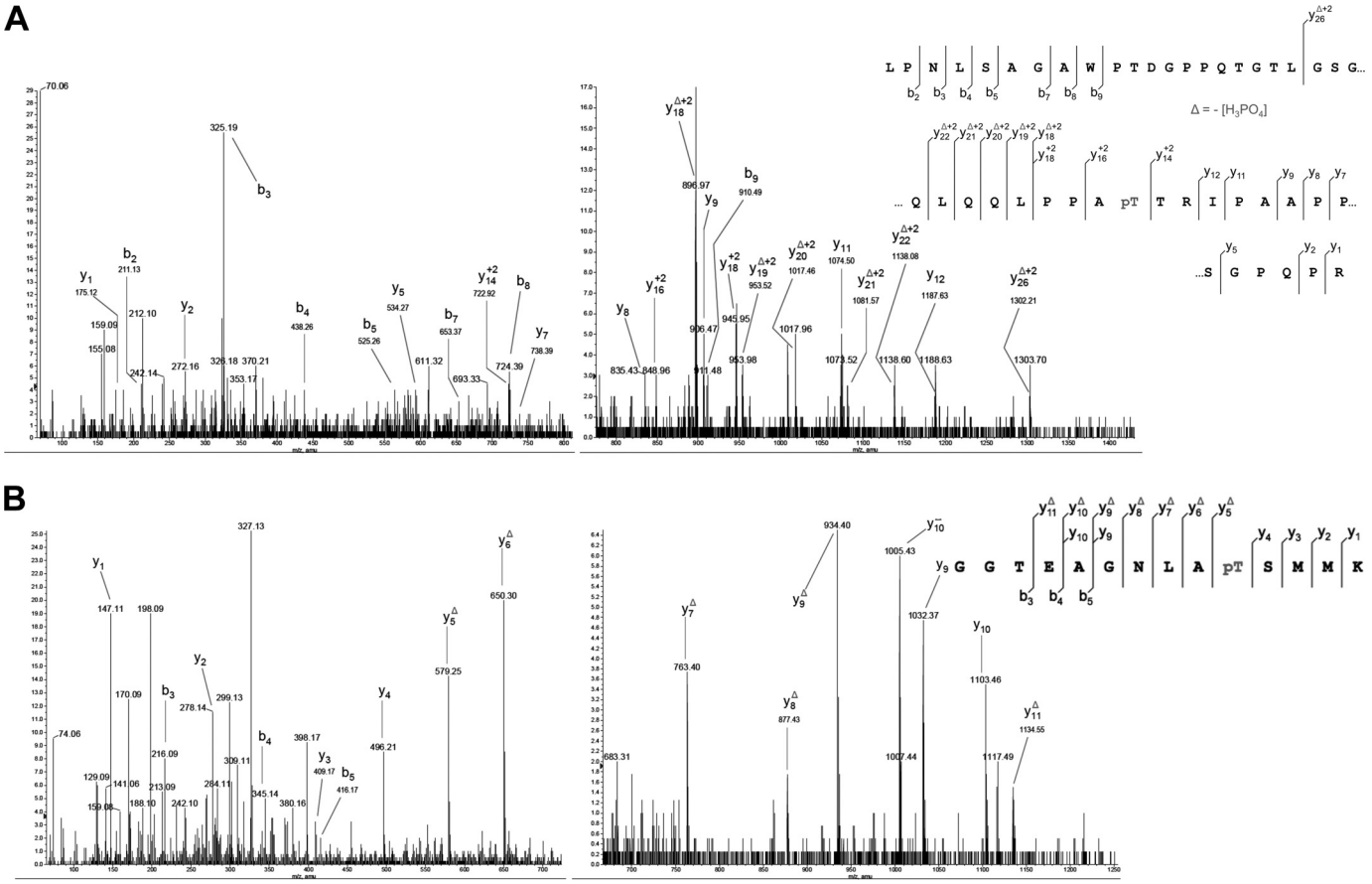

FIGURE 3. **Identification of the Rv1747 phosphorylation sites.** *A,* MS/MS spectra at *m/z* 1170.2 (+4) of peptide 119–164 (monoisotopic mass 4675.44 Da) of Rv1747. Unambiguous location of the phosphate group on Thr-150 was shown by observation of the "y" C-terminal daughter ion series. Starting from the C-terminal residue, all y ions lose phosphoric acid (−98 Da) after the phosphorylated residues. *B,* MS/MS spectra at *m/z* 724.4 (+2) of peptide 199–212 (monoisotopic mass 1446.15 Da) of Rv1747. Unambiguous location of the phosphate group on Thr-208 was shown by observation of the y C-terminal daughter ion series. Starting from the C-terminal residue, all y ions lose phosphoric acid (−98 Da) after the phosphorylated residues.

not co-purified. The phosphorylated Rv1747 isoform was directly analyzed by mass spectrometry as described above, and the MS/MS spectra confirmed the presence of phosphate groups on each of the phosphorylation sites identified previously (data not shown).

Definitive identification of the Thr-150 and Thr-208 residues determined by mass spectrometry was achieved by site-directed mutagenesis by introducing mutations that prevented their specific phosphorylation. Thus, single and double mutations were performed replacing threonine residues by alanine, yielding the mutants Rv1747_T150A, Rv1747_T208A, and Rv1747_T150A/T208A. These mutant proteins were expressed in *E. coli*, purified, and incubated with [γ-^{32}P]ATP and PknF (Fig. 2*B*). Importantly, phosphorylation of the double mutant (phospho-ablative mutant), Rv1747_T150A/T208A, was almost totally abrogated compared with phosphorylation of Rv1747_WT (Fig. 2*B*), indicating that Rv1747 is phosphorylated only on these two residues, at least *in vitro*, in the presence of PknF. This was further supported by analysis of an additional round of mass spectrometry of Rv1747_T150A/T208A pretreated with ATP and PknF, which failed to identify any additional phosphate groups (data not shown). However, as shown in Fig. 2*B*, the T150A or T208A substitutions reduce the phosphorylation signal of the mutants compared with Rv1747_WT but not as much as the double mutant. Taken together, these results indicate that Thr-150 and Thr-208 are the primary targets for PknF phosphorylation *in vitro*, suggesting that they are likely to play critical roles in the regulation of Rv1747 *in vivo*.

*Growth of the Δ*Rv1747* *Mutant and the Phospho-ablative Mutant Strains Was Attenuated in Macrophages and in Mice*—We have previously demonstrated that deletion of *Rv1747* resulted in a growth defect in macrophage and mouse infections (15). Therefore, with the phosphorylation sites identified above, it became possible to investigate the *in vivo* consequences of Thr-150 and Thr-208 phosphorylation on Rv1747 activity. Thus, site-directed mutagenesis was used to introduce a double T150A/T208A mutation into the *Rv1747* complementing plasmid previously used (15), which includes *Rv1747*, *pknF* (*Rv1746*), and 609 bp of *Rv1745* (Fig. 1*A*). This construct was then integrated into the *attB* site of the Δ*Rv1747* mutant to produce a phospho-ablative *Rv1747*-complementing strain. These different strains were used in macrophage and mouse infections. As shown in Figs. 4 and 5, growth of the Δ*Rv1747* strain in BMDMs and in mice was significantly attenuated for growth. In fact, growth of the Δ*Rv1747* mutant was approximately 1 log lower than the WT strain at 168 h post-infection in naive and IFNγ-activated BMDMs (Fig. 4) and was more than 1 log lower in the lungs and almost 4 logs lower in the spleens

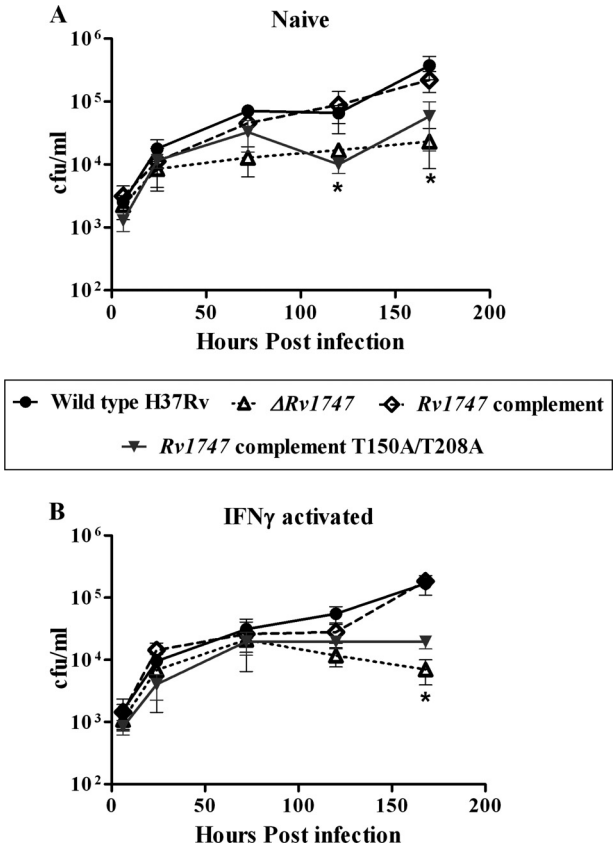

FIGURE 4. **Growth of the strains in macrophages.** Growth of the WT, Δ*Rv1747* mutant, *Rv1747* complement, and *Rv1747* complement T150A/T208A strains over 168 h in naive (*A*) and IFNγ-activated (*B*) macrophages. *Error bars* indicate mean ± S.D. of three technical replicates. *p* values are derived from unpaired Student's *t* tests between the WT and the Δ*Rv1747* or *Rv1747* complement T150A/T208A strains. The *asterisk* indicates that the result is statistically significantly different from that of the WT ($p < 0.05$).

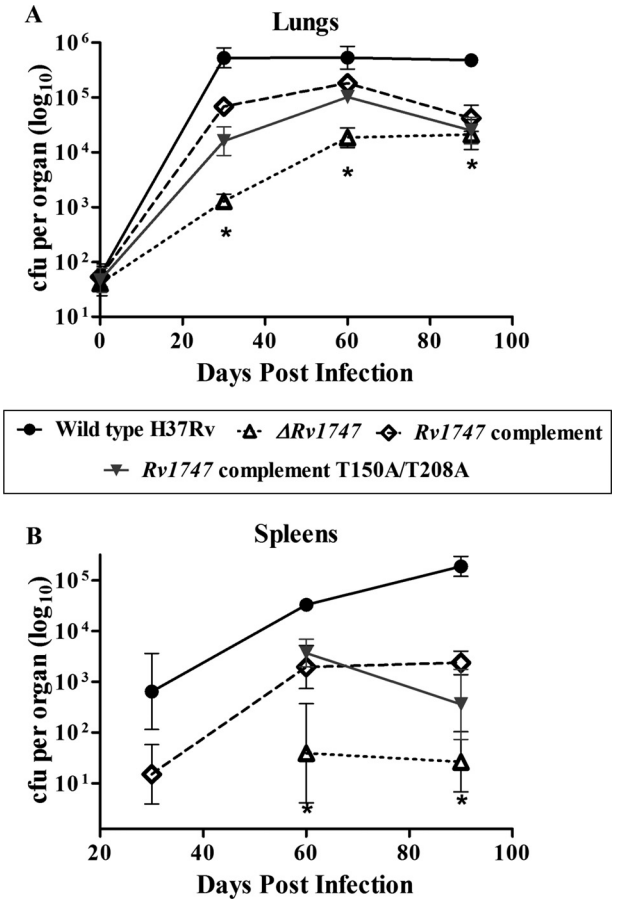

FIGURE 5. **Growth of the strains in mice.** Growth of the WT, Δ*Rv1747* mutant, *Rv1747* complement, and *Rv1747* complement T150A/T208A strains over 90 days in the lungs (*A*) and in the spleens (*B*) of mice. Data for each time point are the means of the cfu determinations performed on organs from five mice, and the *error bars* means ± S.E. At 30 days post-infection, there were no colony-forming units present in the spleens of mice infected with the Δ*Rv1747* mutant or the *Rv1747* T150A/T208A strain. The *asterisk* indicates that the result is statistically significantly different from that of the WT by two-tailed unpaired Student's *t* test ($p < 0.05$).

than the WT strain at 90 days post-infection (Fig. 5). However, growth *in vitro* of the Δ*Rv1747* mutant and the complemented strain, as measured by OD_{600} readings, did not differ from that of the WT strain thus indicating that growth attenuation is specific to the host-pathogen environment and that Rv1747 is critical for growth in macrophages and mice rather than an *in vitro* growth defect (15). Importantly, growth *in vivo* of the T150A/T208A phospho-ablative strain was attenuated, displaying an intermediate growth phenotype between that of the Δ*Rv1747* mutant and WT complement in both BMDMs and in mice (Figs. 4 and 5). These data confirm that phosphorylation of Thr-150 and Thr-208 plays a critical role in positively regulating Rv1747 activity.

Growth of the ΔpknF Mutant Strain Was Not Attenuated in Macrophages—Because of the growth attenuation phenotype observed with the Δ*Rv1747* mutant in both infection models (Figs. 4 and 5) and because PknF phosphorylates Rv1747 (Figs. 2 and 3), it was therefore interesting to investigate the consequences of *pknF* deletion on the growth of *M. tuberculosis* in BMDMs. Growth *in vitro* of the Δ*pknF* mutant and the complemented strain, as measured by OD_{600} readings, did not differ from that of the WT strain (data not shown). As shown in Fig. 6, growth of the Δ*pknF* strain in BMDMs was not significantly different compared with growth of the WT or *pknF* complementing strain (Fig. 6) suggesting that Rv1747 is probably able to be phosphorylated *in vivo* by other STPK(s) when its preferred kinase, PknF, is missing.

FHA-1 Is Required for Rv1747 Function, and Both FHA Domains Bind the Rv1747 Phosphothreonine Epitopes with Similar Affinities—Our *in vivo* assays in macrophages and mice demonstrated that Rv1747 was tightly regulated by phosphorylation. However, the specific role of the Rv1747 FHA domains in Rv1747 regulation by PknF remained to be investigated. The structure of the Rad53 FHA-1 domain from *Saccharomyces cerevisiae* in complex with a phosphothreonine peptide has indicated that there are six highly conserved residues in the FHA domain (31). Five are located around the peptide-binding site, three of which make interactions with the peptide. Of these three, only two, Arg-70 and Ser-85, bind directly to the Thr(P) residue itself and are essential for this interaction. We have therefore mutated the equivalent serine residues in the two FHA domains of Rv1747, Ser-47 in FHA-1 and Ser-248 in FHA-2 to alanines, and generated two additional *Rv1747*-complementing strains. We showed that mutation of FHA-1 results in a growth attenuation phenotype in BMDMs (Fig. 7) suggest-

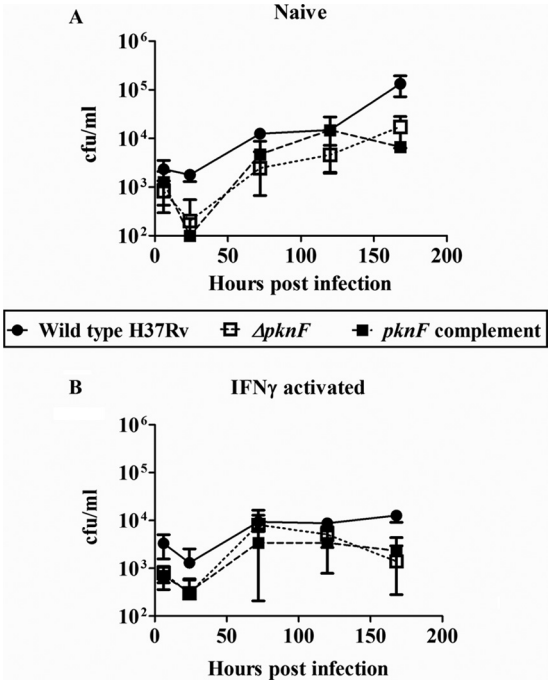

FIGURE 6. **Growth of the *pknF* strains in macrophages.** Growth of the WT, Δ*pknF* mutant, and *pknF* complement strains over 168 h in naive (*A*) and IFNγ-activated (*B*) macrophages. *Error bars* indicate the means ± S.D. of three technical replicates.

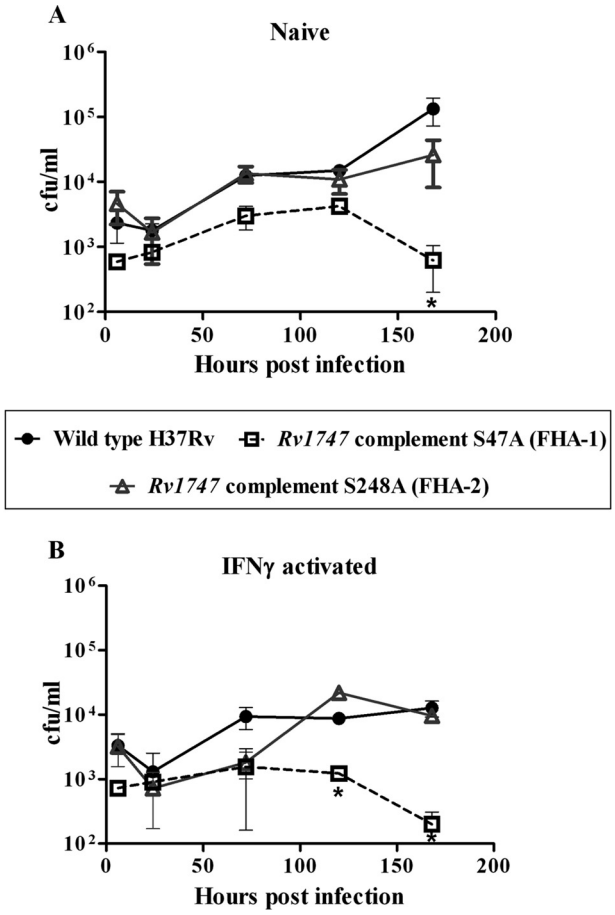

FIGURE 7. **Growth of the FHA domain mutants in macrophages.** Growth of the WT, *Rv1747* complement S47A, and *Rv1747* complement S248A strains over 168 h in naive (*A*) and IFNγ-activated (*B*) macrophages. *Error bars* indicate the means ± S.D. of three technical replicates. *p* values are derived from unpaired Student's *t* tests between the WT and the *Rv1747* complement S47A strains. The *asterisk* indicates that the result is statistically significantly different from that of the WT ($p < 0.05$).

ing that FHA-1 is essential for Rv1747 function. In fact, growth of the FHA-1 mutant was more than 1 log lower than the WT strain at 168 h post-infection in naive and IFNγ-activated BMDMs (Fig. 7). Interestingly, growth of the FHA-2 domain mutant was not significantly different from the growth of the WT strain (Fig. 7) suggesting that this domain is not essential for Rv1747 function.

From these BMDM infections, it therefore appeared interesting to investigate the role of this FHA-1 domain at the molecular level. Moreover, we wanted to determine the binding affinities and stoichiometries between both the Rv1747 FHA domains and the Thr(P)-150 and Thr(P)-208 phosphopeptides to understand more about the interplay between the FHAs and the PknF-phosphorylated motifs within Rv1747 in controlling the Rv1747 signaling system. Using isothermal titration calorimetry, both FHA domains were shown to bind both Rv1747 phosphothreonine epitopes with similar affinities in the micromolar range (Fig. 8). However, the FHA-1 interaction with both the phosphopeptides was abolished upon mutation of Ser-47 to Ala in the peptide binding pocket of FHA-1, thus strongly suggesting that the interactions between the FHA domains and the epitopes are specific. These isothermal titration calorimetry data coupled with the fact that we observed growth attenuation in an FHA-1 S47A mutant (Fig. 7) and in a *Rv1747* T150A/T208A strain in macrophages and mice (Fig. 4 and Fig. 5) allows us to speculate that the FHA domains, particularly FHA-1, play dual roles in Rv1747 regulation through both recruitment of PknF and, potentially, through phospho-dependent interactions with PknF target sites within the dimeric Rv1747 assembly.

DISCUSSION

Reversible phosphorylation is a ubiquitous mechanism of signaling transduction often used to transduce extracellular signals into cellular responses (2). Intriguingly, mycobacterial genomes contain relatively few histidine kinases and response regulators compared with other bacterial genomes of a similar size (32). Although 30 genes encoding putative two-component system proteins have been identified in the *M. tuberculosis* genome (9), only 11 systems paired in operons have been characterized. This is far fewer than in *E. coli* where over 30 pairs have been characterized (33). However, this paucity of histidine kinase-based signal transduction systems in *M. tuberculosis* may be compensated by the relatively large number of STPKs (11) in the genome (8, 9). Therefore, it is thought that in *M. tuberculosis,* STPKs fulfill the role of the classical bacterial two-component systems (8, 32). Interestingly, STPKs have been discovered in many species of pathogenic bacteria, including *Listeria monocytogenes*, *Pseudomonas aeruginosa*, and *Streptococcus pneumoniae* implicating STPKs in the regulation of virulence and pathogenesis of these organisms (34). Furthermore, STPKs are present particularly in organisms such as *Streptomyces*

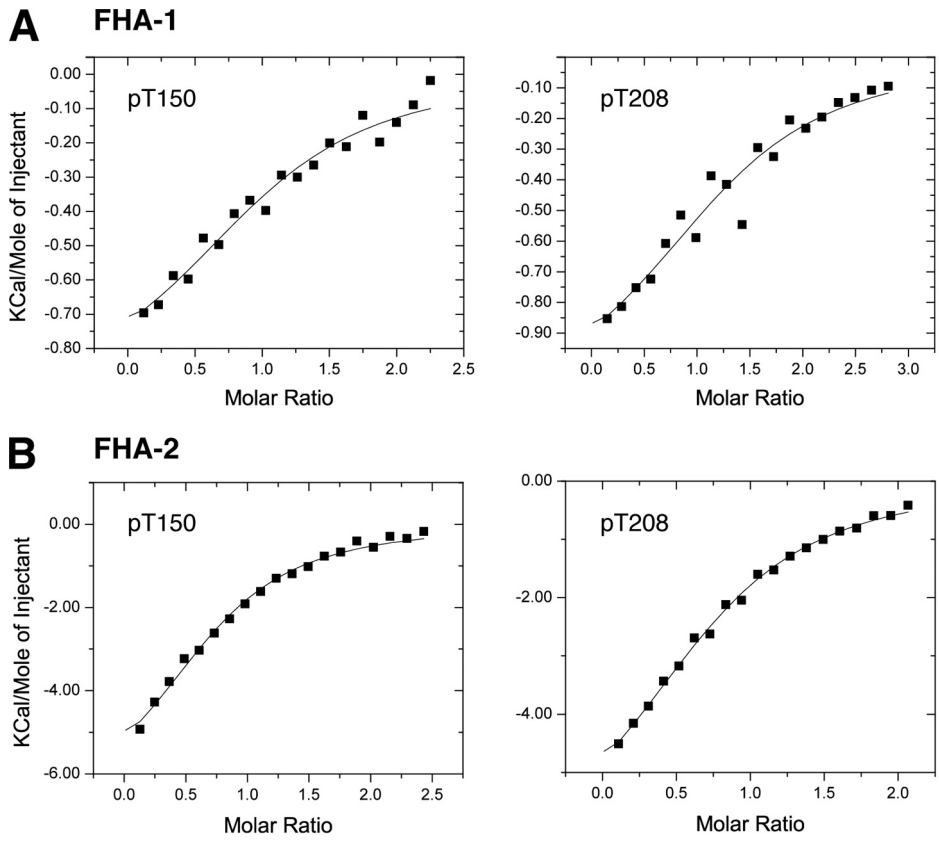

C

Protein	Peptide	Kd (μM)	N	ΔH (kcal/mol)	TΔS (kcal/mol)
FHA1	pT150	2.0	1.04	-0.95	5.15
FHA1	pT208	1.6	1.28	-1.16	5.07
FHA2	pT150	1.6	0.74	-7.07	-0.85
FHA2	pT208	1.8	0.79	-6.76	-0.60
FHA1 S47A	pT150	N. D. B.			
FHA1 S47A	pT208	N. D. B.			

FIGURE 8. **Characterization of FHA domain-phosphopeptide interactions.** Isothermal titration calorimetry (*ITC*) was used to determine the binding kinetics between the FHA domains and the Rv1747 phosphopeptides (denoted as *pT150* and *pT208*). Titrations for FHA-1 (*A*) and FHA-2 (*B*) are shown along with a summary of the thermodynamic parameters (*C*).

where proteins are phosphorylated in response to developmental phases, including secondary metabolism (35). The *M. tuberculosis* STPKs have been implicated to have diverse regulatory effects, and potential functions of some of the proteins have been deduced experimentally (6). For example, PknA and PknB (the two essential STPKs) have been implicated to have roles in cell morphology and shape (36, 37); phosphorylation of Rv1827 by PknB (or PknG) abrogates binding of Rv1827 to three proteins that are all involved in α-ketoglutarate metabolism (38); PknE is involved in the nitric oxide stress response and apoptosis of *M. tuberculosis* in a human macrophage model of infection (39), and PknG promotes mycobacterial survival within macrophages by preventing phagosome-lysosome fusion (40).

Clearly, the *M. tuberculosis* STPK signaling network is highly complex and still rather poorly understood. Here, we have identified two specific threonine residues on Rv1747 that are phosphorylated *in vitro* by PknF and that have *in vivo* modulatory effects on the function of the Rv1747 ABC transporter. We showed that mutation of Thr(P)-150 and Thr(P)-208 results in almost complete loss of phosphorylation of Rv1747 by PknF *in vitro*. This result demonstrated that the two residues identified are both important for PknF phosphorylation of Rv1747, although other minor sites may play additional roles (Fig. 2). We have further investigated the consequences of Rv1747 phosphorylation by assessing the *in vivo* growth of *M. tuberculosis* mutated at these critical Thr residues and showed that growth is attenuated in both BMDMs, as well as in the lungs and spleens of mice. This latter result indicates that phosphorylation of Rv1747 is required for its function, *i.e.* that phosphorylation positively regulates its function. The alternative possibility of negative regulation whereby phosphorylation inhibited Rv1747 function would not be expected to result in growth attenuation of

the Thr-150/Thr-208 mutant and neither would a situation where phosphorylation had no effect on Rv1747 function.

The Δ*pknF* mutant showed no clear growth phenotype in BMDMs thus confirming that Rv1747 is probably able to be phosphorylated *in vivo* by other STPK(s) when its preferred kinase is absent. This point is supported by the fact that PknB can slightly phosphorylate Rv1747, although PknF is clearly more intense *in vitro* (supplemental Fig. S1*A*). Incidentally, a similar result was obtained using 50 μM cold ATP, thus removing the possibility that PknF appears to be the most effective because it has the lowest K_m value for ATP (supplemental Fig. S1*C*). Therefore, one could imagine that *in vivo*, when the preferred PknF kinase is missing, another STPK could phosphorylate Rv1747. The fact that various *M. tuberculosis* STPKs appear able to phosphorylate domains of Rv1747 (16) suggests that its activity might be regulated *in vivo* by multiple environmental signals. This hypothesis is based on observations by different groups that show that mycobacterial Ser/Thr kinases are able to cross-talk and recognize the same substrate *in vitro* (and probably also *in vivo*) (5–7, 16) in order for the mycobacteria to integrate different kinds of signals emitted in distinct environmental conditions.

Furthermore, we have shown that the function of Rv1747 was disrupted by mutation of Ser-47 of FHA-1, which is a highly conserved phospho-interacting residue in FHA domains (31, 41). In contrast, growth of *M. tuberculosis* with mutation of S248A of FHA-2 in BMDMs was the same as the WT. These data greatly strengthen our previous observations that the interaction of Rv1747 with PknF was reduced by 99% by substitution of Ser-47 by Ala in FHA-1 of Rv1747 using yeast two-hybrid analysis but was only approximately one-third reduced by substitution of Ser-248 by Ala in FHA-2 (15). Furthermore, in our previous experiments, phosphorylation of Rv1747 by PknF was reduced to ~5% of the WT levels by substitution of Ser-47 by Ala in FHA-1 and to ~10% of the WT levels by substitution of Ser-248 by Ala in FHA-2 (20), again highlighting the relative importance of both domains.

Taken together, our results suggest that in order for the Rv1747 ABC transporter to function fully, there is a requirement for phosphorylation on residues Thr-150 and Thr-208 that may, in turn, mediate protein-protein interactions with the FHA domains and/or other protein partners to sponsor full Rv1747 activation. Furthermore, our data suggest that Rv1747 must contain a functional FHA-1 domain to mediate interactions with PknF (or other kinases) and/or with Rv1747 itself. The degree of the growth attenuation phenotype of the *Rv1747* complement strain mutated in residues Thr-150 and Thr-208 is not as severe as the growth phenotype seen in the *Rv1747* deletion strain. This indicates that in the absence of phosphorylation on residues Thr-150 and Thr-208 of Rv1747, this ABC transporter can still function to some extent and that phosphorylation serves to positively modulate the transporter. Additionally, our results show that FHA-1 and FHA-2 bind both Thr(P)-150 and Thr(P)-208 phosphopeptides with similar affinities suggesting that *in vivo* both of the FHA domains may be able to bind either of the Thr(P) epitopes to regulate protein function. These interactions could occur within an Rv1747 monomer or across the dimer. Indeed, both intra- and intermolecular regulatory mechanisms have been observed in other FHA domain interactions (38, 42).

A recent study used a mass spectrometry-based approach to identify phosphorylated proteins in *M. tuberculosis* (7). A combined bioinformatic analysis of the *in vivo* phosphorylation sites with data from *in vitro* kinase assays led to identification of phosphorylation site motifs for PknA, PknB, PknD, PknE, PknF, and PknH (7). The motif of the six investigated kinases all included a threonine residue as the phosphoacceptor and hydrophobic residues at the Thr(P)+3 and Thr(P)+5 positions. Residues Thr-150 and Thr-208 of Rv1747 both share some of the features of the PknF preferred phosphorylation motif supporting the identified phosphoacceptor residues as significant in terms of Rv1747 protein function. In fact, the Thr-208 motif has a methionine residue at Thr(P)+3 and an isoleucine residue at Thr(P)+5, both of which appear in the PknF preferred phosphorylation site motif, and the Thr-150 site contains an isoleucine residue at the Thr(P)+3 position, which also appears in the predicted motif (7). Indeed, the FHA domains present in Rv1827 and Rv0020c both select for hydrophobic residues at the Thr(P)+3 position suggesting a common FHA domain recognition mechanism in *M. tuberculosis* that overlaps with that of the STPKs themselves (31, 43).

In conclusion, this work has uncovered significant roles for *pknF* and *Rv1747* genes in *M. tuberculosis* growth *in vivo* and has demonstrated the critical importance of the FHA-1 domain for Rv1747 protein function. However, because the *pknF* mutant has no growth phenotype in an infection, this suggests that this particular kinase would not be a useful target for drug inhibition. Our results suggest that phosphorylation positively modulates the function of the ABC transporter possibly through conformational changes associated with the two FHA domains interacting with Thr(P)-150 and Thr(P)-208 on Rv1747. These data provide evidence for the first time that an STPK can modulate the function of an ABC transporter required for the growth of *M. tuberculosis in vivo*. Future studies are required to determine the PknF stimulus and the precise nature of the phospho-dependent regulatory mechanism of Rv1747 to complete the dissection of this important mycobacterial signaling system.

Acknowledgments—We thank W. Mawby at the University of Bristol for phosphopeptide synthesis and M. Becchi, I. Zanella-Cléon, and A. Cornut (Institut de Biologie et Chimie des Protéines, Lyon, France) for excellent technical assistance in mass spectrometric analysis. We also thank Belinda Dagg, James Keeble, and Biological Services at the National Institute of Biological Standards and Control for help with the mouse infection experiments. We are indebted to Biological Services at the National Institute for Medical Research for animal husbandry and technical support.

REFERENCES

1. Frieden, T. R., Sterling, T. R., Munsiff, S. S., Watt, C. J., and Dye, C. (2003) *Lancet* **362,** 887–899
2. Ubersax, J. A., and Ferrell, J. E., Jr. (2007) *Nat. Rev. Mol. Cell Biol.* **8,** 530–541
3. Hegymegi-Barakonyi, B., Székely, R., Varga, Z., Kiss, R., Borbély, G., Németh, G., Bánhegyi, P., Pató, J., Greff, Z., Horváth, Z., Mészáros, G., Marosfalvi, J., Erôs, D., Szántai-Kis, C., Breza, N., Garavaglia, S., Perozzi, S.,

Rizzi, M., Hafenbradl, D., Ko, M., Av-Gay, Y., Klebl, B. M., Orfi, L., and Kéri, G. (2008) *Curr. Med. Chem.* **15,** 2760–2770
4. Lougheed, K. E., Osborne, S. A., Saxty, B., Whalley, D., Chapman, T., Bouloc, N., Chugh, J., Nott, T. J., Patel, D., Spivey, V. L., Kettleborough, C. A., Bryans, J. S., Taylor, D. L., Smerdon, S. J., and Buxton, R. S. (2011) *Tuberculosis,*
5. Greenstein, A. E., Grundner, C., Echols, N., Gay, L. M., Lombana, T. N., Miecskowski, C. A., Pullen, K. E., Sung, P. Y., and Alber, T. (2005) *J. Mol. Microbiol. Biotechnol.* **9,** 167–181
6. Molle, V., and Kremer, L. (2010) *Mol. Microbiol.* **75,** 1064–1077
7. Prisic, S., Dankwa, S., Schwartz, D., Chou, M. F., Locasale, J. W., Kang, C. M., Bemis, G., Church, G. M., Steen, H., and Husson, R. N. (2010) *Proc. Natl. Acad. Sci. U.S.A.* **107,** 7521–7526
8. Av-Gay, Y., and Everett, M. (2000) *Trends Microbiol.* **8,** 238–244
9. Cole, S. T., Brosch, R., Parkhill, J., Garnier, T., Churcher, C., Harris, D., Gordon, S. V., Eiglmeier, K., Gas, S., Barry, C. E., 3rd, Tekaia, F., Badcock, K., Basham, D., Brown, D., Chillingworth, T., Connor, R., Davies, R., Devlin, K., Feltwell, T., Gentles, S., Hamlin, N., Holroyd, S., Hornsby, T., Jagels, K., Krogh, A., McLean, J., Moule, S., Murphy, L., Oliver, K., Osborne, J., Quail, M. A., Rajandream, M. A., Rogers, J., Rutter, S., Seeger, K., Skelton, J., Squares, R., Squares, S., Sulston, J. E., Taylor, K., Whitehead, S., and Barrell, B. G. (1998) *Nature* **393,** 537–544
10. Hammet, A., Pike, B. L., McNees, C. J., Conlan, L. A., Tenis, N., and Heierhorst, J. (2003) *IUBMB Life* **55,** 23–27
11. Hofmann, K., and Bucher, P. (1995) *Trends Biochem. Sci.* **20,** 347–349
12. Mahajan, A., Yuan, C., Lee, H., Chen, E. S., Wu, P. Y., and Tsai, M. D. (2008) *Sci. Signal.* **1,** re12
13. Durocher, D., and Jackson, S. P. (2002) *FEBS Lett.* **513,** 58–66
14. Braibant, M., Gilot, P., and Content, J. (2000) *FEMS Microbiol. Rev.* **24,** 449–467
15. Curry, J. M., Whalan, R., Hunt, D. M., Gohil, K., Strom, M., Rickman, L., Colston, M. J., Smerdon, S. J., and Buxton, R. S. (2005) *Infect. Immun.* **73,** 4471–4477
16. Grundner, C., Gay, L. M., and Alber, T. (2005) *Protein Sci.* **14,** 1918–1921
17. Canova, M. J., Kremer, L., and Molle, V. (2009) *J. Bacteriol.* **191,** 2876–2883
18. Deol, P., Vohra, R., Saini, A. K., Singh, A., Chandra, H., Chopra, P., Das, T. K., Tyagi, A. K., and Singh, Y. (2005) *J. Bacteriol.* **187,** 3415–3420
19. Gopalaswamy, R., Narayanan, S., Jacobs, W. R., Jr., and Av-Gay, Y. (2008) *FEMS Microbiol. Lett.* **278,** 121–127
20. Molle, V., Soulat, D., Jault, J. M., Grangeasse, C., Cozzone, A. J., and Prost, J. F. (2004) *FEMS Microbiol. Lett.* **234,** 215–223
21. Fiuza, M., Canova, M. J., Zanella-Cléon, I., Becchi, M., Cozzone, A. J., Mateos, L. M., Kremer, L., Gil, J. A., and Molle, V. (2008) *J. Biol. Chem.* **283,** 18099–18112
22. Parish, T., and Stoker, N. G. (2000) *Microbiology* **146,** 1969–1975
23. Rickman, L., Scott, C., Hunt, D. M., Hutchinson, T., Menéndez, M. C., Whalan, R., Hinds, J., Colston, M. J., Green, J., and Buxton, R. S. (2005) *Mol. Microbiol.* **56,** 1274–1286
24. Kong, D., and Kunimoto, D. Y. (1995) *Infect. Immun.* **63,** 799–803
25. Springer, B., Sander, P., Sedlacek, L., Ellrott, K., and Böttger, E. C. (2001) *Int. J. Med. Microbiol.* **290,** 669–675
26. Cohen-Gonsaud, M., Barthe, P., Canova, M. J., Stagier-Simon, C., Kremer, L., Roumestand, C., and Molle, V. (2009) *J. Biol. Chem.* **284,** 19290–19300
27. Molle, V., Gulten, G., Vilchèze, C., Veyron-Churlet, R., Zanella-Cléon, I., Sacchettini, J. C., Jacobs, W. R., Jr., and Kremer, L. (2010) *Mol. Microbiol.* **78,** 1591–1605
28. Veyron-Churlet, R., Molle, V., Taylor, R. C., Brown, A. K., Besra, G. S., Zanella-Cléon, I., Fütterer, K., and Kremer, L. (2009) *J. Biol. Chem.* **284,** 6414–6424
29. Veyron-Churlet, R., Zanella-Cléon, I., Cohen-Gonsaud, M., Molle, V., and Kremer, L. (2010) *J. Biol. Chem.* **285,** 12714–12725
30. Molle, V., Leiba, J., Zanella-Cléon, I., Becchi, M., and Kremer, L. (2010) *Proteomics* **10,** 3910–3915
31. Durocher, D., Taylor, I. A., Sarbassova, D., Haire, L. F., Westcott, S. L., Jackson, S. P., Smerdon, S. J., and Yaffe, M. B. (2000) *Mol. Cell* **6,** 1169–1182
32. Wehenkel, A., Bellinzoni, M., Graña, M., Duran, R., Villarino, A., Fernandez, P., Andre-Leroux, G., England, P., Takiff, H., Cerveñansky, C., Cole, S. T., and Alzari, P. M. (2008) *Biochim. Biophys. Acta* **1784,** 193–202
33. Mizuno, T. (1997) *DNA Res.* **4,** 161–168
34. Cozzone, A. J. (2005) *J. Mol. Microbiol. Biotechnol.* **9,** 198–213
35. Umeyama, T., Lee, P. C., and Horinouchi, S. (2002) *Appl. Microbiol. Biotechnol.* **59,** 419–425
36. Dasgupta, A., Datta, P., Kundu, M., and Basu, J. (2006) *Microbiology* **152,** 493–504
37. Kang, C. M., Abbott, D. W., Park, S. T., Dascher, C. C., Cantley, L. C., and Husson, R. N. (2005) *Genes Dev.* **19,** 1692–1704
38. Nott, T. J., Kelly, G., Stach, L., Li, J., Westcott, S., Patel, D., Hunt, D. M., Howell, S., Buxton, R. S., O'Hare, H. M., and Smerdon, S. J. (2009) *Sci. Signal.* **2,** ra12
39. Jayakumar, D., Jacobs, W. R., Jr., and Narayanan, S. (2008) *Cell. Microbiol.* **10,** 365–374
40. Walburger, A., Koul, A., Ferrari, G., Nguyen, L., Prescianotto-Baschong, C., Huygen, K., Klebl, B., Thompson, C., Bacher, G., and Pieters, J. (2004) *Science* **304,** 1800–1804
41. Li, J., Williams, B. L., Haire, L. F., Goldberg, M., Wilker, E., Durocher, D., Yaffe, M. B., Jackson, S. P., and Smerdon, S. J. (2002) *Mol. Cell* **9,** 1045–1054
42. Li, J., Taylor, I. A., Lloyd, J., Clapperton, J. A., Howell, S., MacMillan, D., and Smerdon, S. J. (2008) *J. Biol. Chem.* **283,** 36019–36030
43. Pennell, S., Westcott, S., Ortiz-Lombardía, M., Patel, D., Li, J., Nott, T. J., Mohammed, D., Buxton, R. S., Yaffe, M. B., Verma, C., and Smerdon, S. J. (2010) *Structure* **18,** 1587–1595
44. Amrein, K. E., Takacs, B., Stieger, M., Molnos, J., Flint, N. A., and Burn, P. (1995) *Proc. Natl. Acad. Sci. U.S.A.* **92,** 1048–1052
45. Oatway, W. H., Jr., and Steenken, W. (1936) *J. Infect. Dis.* **59,** 306–325
46. Papavinasasundaram, K. G., Anderson, C., Brooks, P. C., Thomas, N. A., Movahedzadeh, F., Jenner, P. J., Colston, M. J., and Davis, E. O. (2001) *Microbiology* **147,** 3271–3279